Journal of Sustainable Development of Smart Energy Networks

http://www.sdewes.org/jsdsen

Year 2026, Volume 1, Issue 2, 2030690

Original Research Article

Decentralized Hydrogen Refuelling Station Concept: Achieving Security of Supply through Geothermally-Powered Onsite Biomethane Pyrolysis

Kristóf Kummer*[*1], Réka Kustán[1], Attila R. Imre[1,2]

[1]Department of Energy Engineering, Budapest University of Technology and Economics, Budapest, Hungary
[2]Department of Nuclear Safety, HUN-REN Centre for Energy Research, P.O. Box 49, Budapest, Hungary
e–mail: kummer@energia.bme.hu, kustan@energia.bme.hu, imreattila@energia.bme.hu

Cite as: Kummer, K. f., Kustán, R., Imre, A. R., Decentralized Hydrogen Refuelling Station Concept: Achieving Security of Supply through Geothermally-Powered Onsite Biomethane Pyrolysis, J. sustain. dev. smart. en. net., 1(2), 2030690, 2026, DOI: https://doi.org/10.13044/j.sdsen.d3.0690

ABSTRACT

Hydrogen technologies in transport are expanding, yet their growth remains significantly slower than that of battery-electric vehicles due to and demand-side inertia. At low market penetration, the limited number of fuel-cell vehicles restricts the development of a viable refueling network. A promising pathway is decentralized, on-site hydrogen production, which avoids the high upfront investment of centralized systems. Feasibility can be enhanced by methane splitting (MS) using biomethane from existing biogas plants to supply stations along the Hungarian TEN-T corridor and other major motorways. This study examines a representative node near Szarvas, adjacent to the M44 highway, where geothermal energy – via an ORC system – could provide over 1000 kW_{el} of electricity, with residual heat supporting district heating. The analysis applies a comprehensive material and energy balance to perform an LCOH calculation incorporating demand-side hydrogen use, evaluating three scenarios supported by a simplified carbon-intensity assessment.

KEYWORDS

Biomethane splitting, Pyrolysis, Geothermal, Hydrogen mobility, Hydrogen refuelling station, Onsite hydrogen production.

INTRODUCTION

Hydrogen mobility could be a realistic alternative for the transport sector if the parties involved work together or individually to overcome some or all of the currently identified problems and find solutions that could even accelerate the adoption of hydrogen-based transport [1]. Hydrogen's role in road transport is complex [2] due to numerous challenges and competition from both traditional fossil fuels (diesel, gasoline) and low-emission alternatives (such as electric vehicles and compressed natural gas of biological origin). Alreshidi et al. [3] present a comprehensive study highlighting the main difficulties and obstacles facing hydrogen as a fuel. They note that hydrogen production and storage remain highly energy-intensive and economically burdensome, and the predominant production pathway – steam methane reforming (SMR) – still results in substantial CO_2 emissions, thereby limiting the overall environmental benefits of hydrogen. Furthermore, the authors emphasize that the current scarcity of hydrogen refueling infrastructure significantly

* Corresponding author

constrains market growth and inhibits broader consumer uptake. They also highlight persistent technical challenges associated with achieving safe, high-density storage, including the need for high-pressure systems, cryogenic conditions, and materials capable of resisting degradation, all of which present considerable obstacles to widespread deployment in the transport sector. Authors' recent work [4] demonstrated that onsite hydrogen production (electrolysis and methane splitting) can reduce the levelized cost of hydrogen (LCOH) compared to centralized production, and the advantages of MS technology were also presented. Perna *et al.* [5] examined various types of onsite hydrogen production technologies from a techno-economic perspective, which they linked to a Hydrogen Refuelling Station (HRS). Kondor [6] examined the location of Hungarian biogas plants in the country and emphasized those that would be capable of producing biomethane for supplying theoretical HRS. Gianone [7] has already conducted a preliminary assessment of the potential utilisation of geothermal wells in Hungary, with particular emphasis on the well located in Szarvas. Kisari [8] conducted a detailed study on the material and energy balance of the biogas plant in Szarvas, examining the quality and availability of feedstocks as well as the plant's configuration and product portfolio. In this current layout the utilized technology was assessed in detail by Timmerberg *et al.* [9], [10] and Bulfaro *et al.* [10] from categorization perspective. Lee *et al.* [11] placed considerable emphasis on the description and characterisation of the carbon by-products. Their study demonstrates how the formation of specific carbon products depends on the operational characteristics of the reactors. In this article, LCOH calculation was also discussed as an appropriate basis for comparison for economic evaluation.

This paper presents a case study in which the location of the HRS is chosen based on the material and energy flows that supply it. This means that the MS technology capable of producing low-carbon hydrogen is directly connected to the HRS, but the biomethane and renewable energy required for this are also sourced from the immediate vicinity. Based on these considerations, the biogas plant in Szarvas (a mid-size town, in the South-Eastern part of Hungary), located next to the East-West oriented M44 motorway, was selected, which is currently not capable of producing biomethane, since the plant is not equipped with a biogas upgrader unit. However, global trends show, and forecasts confirm, that biomethane will play a greater role than biogas in the future, meaning that carbon dioxide (CO_2) separation (also known as biogas upgrade) will become a key factor [12]. Our analysis focuses on HRS concepts that exclusively serve heavy-duty vehicles (HDVs) with hydrogen (fuel-cell-powered or dual-fueled), as public opinion on mobility and industry reports suggest that hydrogen propulsion is unlikely to penetrate the passenger car market. For this reason, it is worth locating these HRSs in high-traffic areas, mostly frequented by trucks and buses, or even at specific sites such as a city bus depot [13], where these vehicles return every day and refueling can be carried out without any problems. According to our assumption the M44 will play an important role in European road transport in the future [14], as will be discussed in more detail below. Another advantage of the chosen location is the presence of an operational geothermal well, which has the potential to provide heat for a geothermal ORC power plant to produce clean, constant amounts of electricity that is largely independent of weather conditions; this power plant is still in the planning stage [15]. The overall layout also includes an ORC designed to utilize waste heat from the high-temperature MS technology, thereby reducing the plant's overall electricity consumption. Since HRS supplies fuel in the form of hydrogen, the constant production of MS technology is critical from a supply security perspective if large amounts of hydrogen buffer capacity, even tens of tons, are to be avoided. This could happen if we relied solely on solar and wind energy sources, as the phenomenon of "Dunkelflaute" can occur countless times a year, when these renewable solar power plants are unable to generate electricity for weeks at a time [16]. Electrolysis technology could also be used to produce low-carbon hydrogen with a constant source of electricity, but its low

efficiency means that LCOH values are higher even with lower electricity costs [4], [17]. Furthermore, the electricity consumption of electrolysis is at least 4-5 times greater than that of MS technology, which would be challenging to supply with the existing geothermal well.

This study supplements the hydrogen mobility literature by assessing the integration of methane splitting based on-site and small-scale hydrogen production with HRS, a system configuration not previously investigated in scientific or engineering research. The analysis further contributes novelty by jointly considering biomethane as the primary feedstock and geothermal electricity as the energy source – an integrated resource pathway absent from earlier techno-economic assessments. Moreover, the study establishes a complete material and energy balance to derive the LCOH, thereby quantifying one of the most critical techno-economic indicators for emerging hydrogen technologies. By situating the case study within the Hungarian transport and energy context, the research provides region-specific insight, particularly relevant given Hungary's extensive and mature natural gas infrastructure, which offers strategic advantages for transporting easily handled molecules (methane in this particular case) and enabling hydrogen conversion at the point of use. The scenario analysis further demonstrates how variations in technological parameters, economic conditions, and policy frameworks influence the competitiveness of low-carbon hydrogen relative to diesel in heavy-duty transport. This highlights the engineering significance of decentralized hydrogen production as a strategy to tackle infrastructure-related limitations while minimizing the logistical burdens associated with long-distance hydrogen transport.

The current work had three main objectives. First, to present the concept of an onsite MS-based HRS powered by biomethane and geothermal energy, which could offer a real alternative to hydrogen mobility, which is currently stagnating. Second, to examine the necessary parameters and capacities, analyze the technology, identify the main material and energy flows, and define the necessary equipment. Third, to examine the economic feasibility of the entire concept, we sought to answer the question of what challenges the envisioned concept might pose from a business perspective under these circumstances. The justification for the concept was supported by a simplified greenhouse gas (GHG) emissions analysis, in which the GHG emissions of each fuel examined were analyzed for 100 km under different scenarios. The studies mentioned above are presented in the following sections.

METHOD

The investigated layout is shown in **Figure 1**. The scope of the work contains five major units which are responsible for a certain task through the whole technology chain. In the next sections each unit was investigated and presented with material and energy balances, the justification of the selected technologies and highlight of the advantages of the concept.

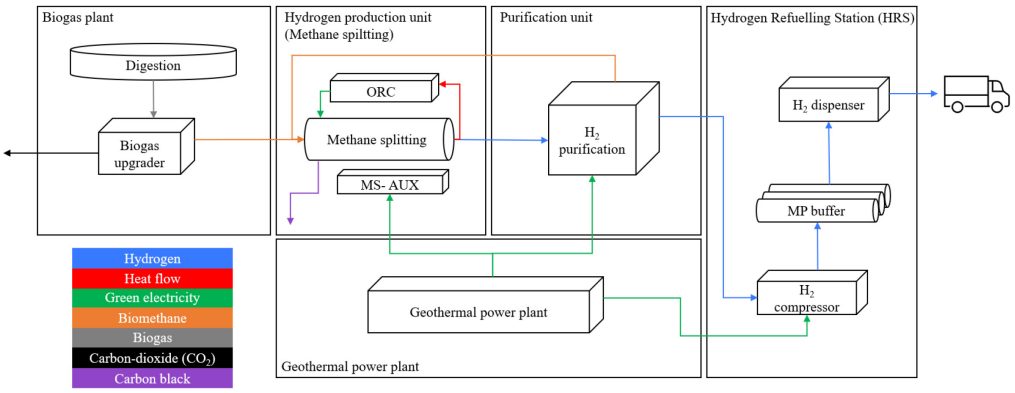

Figure 1. The assessed layout and scope of this work

Biogas Plant and Upgrade

In order to examine the above-mentioned concept, a biogas plant is needed that is located close enough to a busy national highway or motorway and can provide the necessary amount of feedstock for hydrogen production. Kondor examined the location of Hungarian biogas plants in the country in his MSc thesis [6], and the National Biomethane-Biogas Green Energy Industry Association (originally named the National Biomethane-Biogas Green Energy Industry Association) also has a database listing biogas plants with electricity production licenses (the association is a member of the European Biogas Association) [18]. However, these databases do not provide detailed information on the technological details, material and energy flows of the biogas plants in question, and the scientific literature is also very limited in terms of providing accurate information on the characteristics of the plants. The main reason for this is the insistence on trade secrets, which the companies use to protect their competitiveness.

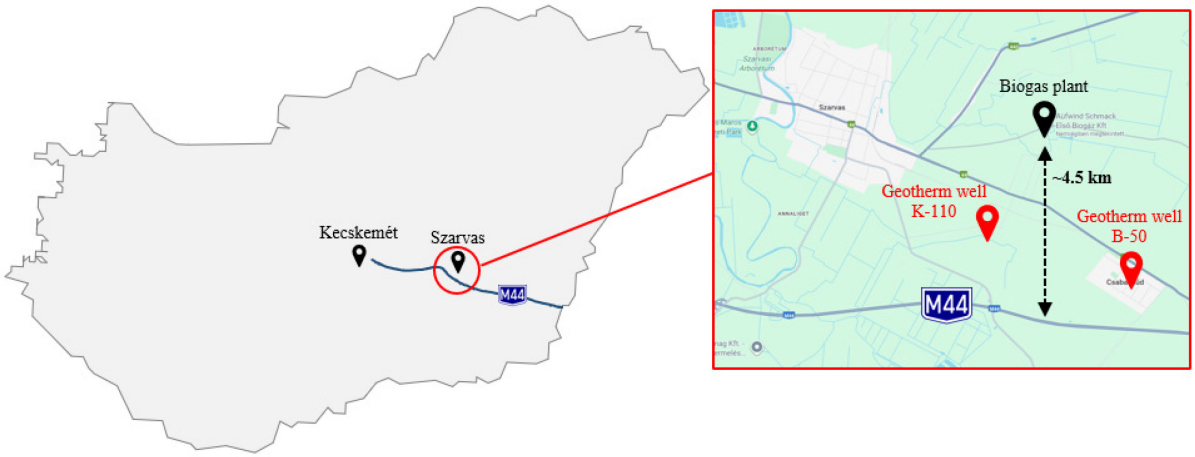

Figure 2. Hungarian highway M44 and the location of biogas plant in Szarvas

One of the largest biogas plants in Hungary is located in Szarvas, owned by MOL Plc. since 2023 (Aufwind Schmack Első Biogáz Ltd.), with an estimated annual biogas yield of 11 – 12 million normal cubic meter (Nm^3). It is located in the south-eastern part of the country, near the M44 motorway, 4.5 km away as the crow flies (**Figure 2**). The plant mainly processes biomass of animal origin, animal manure and waste, but a small proportion of plant-based biomass is also fed into the fermentors [8]. The estimated and calculated data for the biogas plant are summarized in **Table 1**, but it should be noted that it is currently not capable of producing biomethane; the estimated biomethane yield only expresses the potential, not the actual production. This amount is sufficient to supply three HRS units approximately, each with a capacity of 1 t/d, as 1460 tons of biomethane are required to feed such an HRS, taking into account the stoichiometric ratio (4 tons of methane are required for 1 ton of hydrogen). Although the M44 highway near the Szarvas biogas plant is not currently part of the TEN-T road network (Trans-European Transport Network) and is therefore not subject to the EU directive on HRS installations [13], it could become an important element of European transport corridors in the future, both for the Rhine-Danube and the Orient/East-Med Road Corridor [14].

Table 1. Estimated and calculated operational data of Szarvas biogas plant

Estimated annual biogas production	**million Nm^3**		**11 – 12**
Estimated biomethane content of the biogas	vol%		55 – 60
Estimated annual biomethane production potential	million Nm^3		6 – 7
Density of the methane at normal state	kg/Nm^3		0.716
Estimated annual biomethane production potential	kilotonnes		4.3 – 5
Feedstock	mainly manure, small quantity of plant-based biomass		
Biomethane need for an 1 t/d HRS	kilotonnes	1.46	based on material balance

Geothermal Power Plant

There are several locations in Hungary and in general, in the Pannonian basin, where existing geothermal wells could provide heat and electricity at a rate depending on the actual demand and on heat and electricity prices. Unfortunately, only a few of them are used to produce electricity [15], using small or micro power plants based on ORC technology. A preliminary study [7] has been conducted for the Szarvas (a medium-sized town) K-110 well, located close to the neighbouring Csabacsüd (a medium-sized village), where the potential injection well (Csabacsüd B-50, presently unused) is located (see **Figure 2**). Additionally, the distance of Szarvas (a medium-sized town with an existing district heating network) is also not significant, and the well is located close to the line connecting the Szarvas Biogas plant to the M44 highway. Presently, the district heating system of Szarvas needs 500 GJ/year, but the company is willing to extend the covered area; therefore, additional heat sources would easily be utilized. The capacity of the Szarvas K-110 well (currently 98 °C thermal water inlet temperature, which can easily be enhanced by increasing the depth of the well to 120 – 125 °C, a maximum of 80 l/s volume flow) would simply satisfy the heating demand, and the remaining heat could be used to generate electric power. Although these temperatures seem to be low, ORC technology can use them for power production; one good example is the Tura Power Plant in Hungary, with 3.35 MW_e installed capacity, using thermal water with a maximum temperature of around 120 °C [15], [19]. As shown in a recent review, ORC technology – by selecting a suitable expander and working fluid pair – can be used for power production with heat sources well below 100 °C [20]. These devices are not only for laboratory use; they are already available to companies for power production [21]. Due to their compactness (they can be transported to the given location and installed into the existing geothermal system in days), these units are air-cooled. The system could provide the required electric power as well as enough heat for the district heating system. Although the total power production is relatively small, considering the fact that the system would be installed on existing geothermal wells, the Return on Investment (ROI) time would not be extremely long.

For the methane splitting, an ORC device was utilized, generating electricity from geothermal heat [22]. The temperature of the heat source is estimated to be 98 °C, and its mass flow is 93 kg/s; therefore, 10.49 MW_{th} can be utilized from the heat source. The ORC design used during the simulation can be seen in **Figure 3**. On the figure, EVAP refers to the evaporator, the ECO to the liquid heater (economiser), and the R to the recuperative heat

exchanger. The working fluid for this setup is Butane. With this design, 1.18 MW_e power is achievable to supply the methane splitting. This amount of power is enough for the methane splitting process with the auxiliaries, hydrogen purification, and compression unit. The total electricity consumption of the plant could be mitigated with waste heat recovery (see the next Section), therefore, the total plant consumption could be decreased to 1.17 MW_e from 1.28 MW_e. In the section of the Economic analysis is presented that the electricity supply cost was calculated by unit cost of the geothermal electricity [23] instead of the calculation of new investment such as an ORC unit deployment next to the geothermal well. This results conservative calculation due to the fact that our layout does not require drilling of new geothermal well, although the unit cost contains this element.

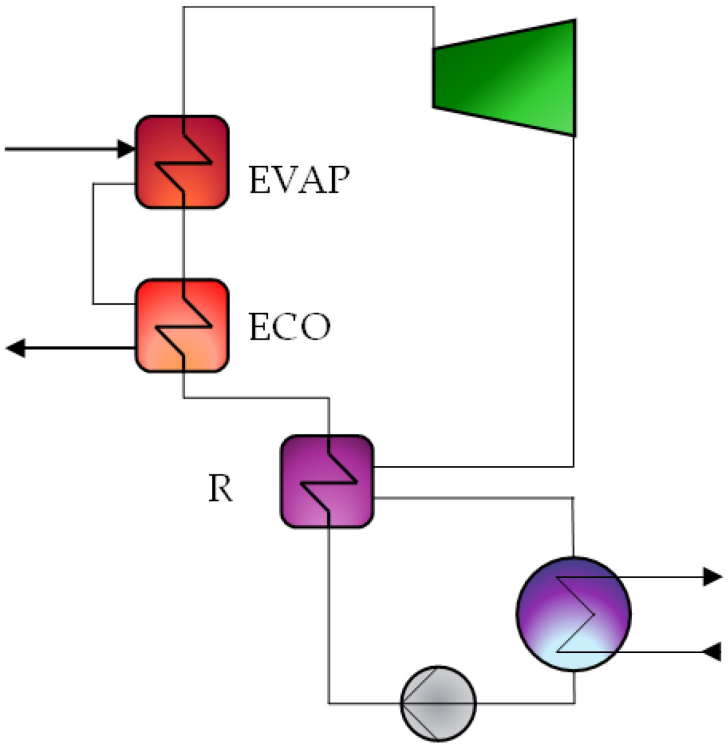

Figure 3. ORC design for geothermal use and waste heat recovery

Methane Splitting

The central element of the technological line under investigation is the hydrogen production plant, which produces hydrogen from (bio)methane and electricity as a raw material for HRS, as well as valuable solid carbon by-products. Methane splitting, also known as methane pyrolysis or methane cracking, is an emerging and increasingly researched technology in which the C-H covalent bonds in methane are broken down in such a way that no oxidized carbon, carbon monoxide or carbon dioxide is produced as a by-product, but rather elemental carbon is formed. The reaction is endothermic, so the energy required to break the bonds must be supplied from an external source. Timmerberg *et al.* have provided a transparent and comprehensive classification of reactors and catalysts according to the type of catalyst and the source of energy supplied [9]. The number of publications on methane splitting is constantly growing. Publications related to the technology and its evaluation are listed in **Table 2**. A more detailed description of the technology itself is already under publication [4]. Since the goal is to prepare a specific case study, the following section analyzes and discusses these quantities and properties together. The case study analyzes plasma-based technology, specifically the non-thermal plasma type.

Table 2. Significant literatures related the specific segments of methane splitting

Technology fundamentals of the methane splitting technology	**Patlolla *et al.* [24]**
Types of the methane splitting	Timmerberg *et al.* [9] Bulfaro *et al.* [10]
Classification and examination of carbon product	Lee *et al.* [11]
Technology maturity of the methane splitting technologies	Kummer and Imre [4]
Environmental, economic, and social impacts of methane splitting	Bulfaro *et al.* [10]
Techno-economic analysis	Pérez *et al.* [25]

The MS unit, which can be integrated into the technological line, was dimensioned based on the amount of hydrogen required by the HRS. The daily quantity of 1 ton corresponds to a hydrogen flow of 41.7 kg/h, which must be produced by the MS technology. In this case, however, annual availability would have to be 100% (8760 hours/year), which is practically unachievable with any technology, especially one at Technology Readiness Level 6-9 (TRL). For this reason, the nominal hydrogen production capacity of the MS technology was set at 50 kg/h, thus avoiding the problem of the HRS not having enough hydrogen every day of the year. In terms of input flows, the mass flow of methane is 200 kg/h, in accordance with the stoichiometric equation. A circulated methane stream will be discussed in detail later, which remains as a contaminant alongside hydrogen and is returned to the MS as a raw material after the purification sub-technology. The MS's electricity consumption consists of two parts: on the one hand, the amount required for the reaction, which was calculated based on a specific electricity consumption of 10 kWh/kg H_2, taking into account that the chosen technology is non-thermal plasma MS. On the other hand, auxiliary and downstream equipment also consume electricity, such as pumps, compressors, product coolers, etc. Their consumption was treated collectively, with a total value of 4 kWh/kg H_2 [9].

The mass flow rate of solid carbon, considered a valuable by-product, is 150 kg/h, which in this case study is carbon black (CB). However, with careful selection of technology, correct adjustment of reactor parameters, and selection of the type of post-treatment, higher-value carbon can also be obtained (graphite, graphene, nanostructured graphene) [11]. Since the aim of the case study is to provide HRS with hydrogen of the appropriate quality and quantity, it would not be advisable for our economic calculations to be dominated entirely by the revenue from carbon sales. A report by Dagle *et al.* analyzed the current and future price ranges of individual carbon products [26]. According to the report, a higher-value product (e.g., carbon fiber) can range from USD 20,000 to USD 113,000 per ton in certain industries, which in our case would completely distort the purpose of the study, as hydrogen itself would be the by-product. Therefore, we estimated the price of carbon conservatively in our economic calculations.

Waste heat released from the technology, which can be obtained from cooling high-temperature products, should also be treated as a by-product. In our calculations, we assumed a reactor temperature of 1000 °C, so waste heat is potentially available at this temperature at the product heat exchanger. Its quantity can be calculated from the energy balance, where the input flows are methane and electricity (only required for the reaction), and the output flows are hydrogen and CB. The difference between these is the potentially usable waste heat, which is 0.464 MW for a plant with a hydrogen production capacity of 50 kg/h. For methane, hydrogen and CB, the energy flow was calculated using the lower heating value (LHV). The characteristic data used for the MS plant case study are shown in **Table 3**.

Table 3. Main characteristics of the hydrogen production unit (the methane splitting unit)

Utilization rate	**-**	**h/year**	**7588**	
Reactor type	-	-	non-thermal plasma	
Reactor temperature	$T_{reactor}$	°C	1000	[10]
Pressure of the reactor	$p_{reactor}$	bar	1.8	[25]
Nominal mass flow of the methane stream	$\dot{m}_{CH4}$	kg/h	200	
Total input methane stream to MS	$\dot{m}_{CH4,tracer} + \dot{m}_{CH4}$	kg/h	208.2	
Lower heating value of the methane	LHV_{CH4}	MJ/kg	50	at 1bar, 15°C
Energy flow of the methane stream	P_{CH4}	MW	2.89	
Specific electricity consumption of the splitting process	e_{proc}	kWh/kg H_2	10	[9]
Power for the splitting process	$P_{elec,proc}$	MW	0.5	
Specific electricity consumption of the auxiliaries of MS	e_{aux}	kWh/kg H_2	4	[9]
Power for the auxiliaries	$P_{elec,aux}$	MW	0.2	
Temperature of the waste heat	T_{waste}	°C	1000	[10]
Power of the waste heat	P_{waste}	MW	0.464	calculated based on the energy balance
Mass flow of the carbon black	$\dot{m}_{CB}$	kg/h	150	
Energy density of CB	e_{CB}	MJ/kg	27.5	
Energy flow of the CB	P_{CB}	MW	1.1	
Nominal mass flow of the hydrogen	$\dot{m}_{H2}$	kg/h	50	
Nominal mass flow of the methane as tracer	$\dot{m}_{CH4,tracer}$	kg/h	8.2	
Nominal mass flow of the gas mixture product	$\dot{m}_{H2,pur,in} = \dot{m}_{CH4,tracer} + \dot{m}_{H2}$	kg/h	58.2	
Purity of the hydrogen after MS	p_{H2}	vol%	98	

For the better viability of the method, we should recover some of the waste heat generated during the process of methane splitting [27]. It can be said that this is "good quality" (high temperature) heat, which can be used for power generation with higher efficiency. The temperature at which the waste heat is available during the methane splitting process is 1000 °C, and this way, it is possible to recover 0.464 MW_{th} heat with an ORC while generating 0.11 MW_e. The used ORC design is the same as the one used for the geothermal source (**Figure 3**); however, the working fluid in this case is toluene to better match the heat source temperature during the heat recovery. In this way, 0.11 MWe power was produced, and therefore the power needed for the total process (including the methane splitting and the gas compression) can be reduced by this amount. Based on Pantaleo *et al.* [28] the ORC CAPEX cost was calculated with 3000 EUR/kW_e which is shown in our economic analysis below.

Hydrogen Purification

Since the hydrogen produced after MS is not fuel cell-grade, it must be purified, assuming that the only contaminant besides hydrogen is unreacted methane. The mass flow rate entering the purification unit is 58.2 kg/h, of which 50 kg/h is hydrogen and 8.2 kg/h is methane. The available technologies offer a number of different solutions depending on the intended use. The oldest and most reliable technology for this task is Pressure Swing Absorption (PSA), which is the most common method of hydrogen purification in traditional industries (e.g., oil refining, chemical industry). These are ideal for large-volume hydrogen streams; for smaller quantities, it is better to consider other alternatives [29]. In the current work, we have been searching for a hydrogen purification technology developed for low-capacity, decentralized applications with the lowest possible operating costs. In addition to the above conditions, high availability and reliability are important factors, as filling stations require a continuous flow of material. Król *et al.* [30], compared different hydrogen purification technologies, using the method of hydrogen use and the individual production processes as a basis for comparison. The characteristics that are important to us can be found in polymer membrane purification [31] so this type was used as a basis in the technology line. The advantages of membrane-based technologies are their compact design, simple operation, low energy consumption, and low environmental impact, but they can be sensitive to certain contaminants, which in extreme cases can mean the end of the membrane's life [32]. New membrane technologies such as carbon molecule sieve membranes (CMSMs) [33], ionic liquid membranes [34] and electrochemical pump membranes [35] may be promising alternatives among hydrogen technologies, but these are mostly available in laboratory or pilot scale [32]. Arias *et al.* studied membrane separation processes in an oil refinery environment [36], which show that a single purification stage is not sufficient to achieve the 99.97 vol% hydrogen composition we require; a minimum two-stage cascade membrane process is necessary to achieve the desired purity [37]. The required pressure is generated by piston hydrogen compressors upstream of the first and second membranes. According to current assumptions, the gas mixture to be purified contains only methane, so only methane appears on the retentate side (residue), which must be taken care of, as it cannot be released into the atmosphere due to its greenhouse effect [38]. To this end, the methane retentate is fed back into the methane splitting reactor. Alternatively, it could also be burned in a combined heat and power (CHP) unit, thereby increasing the efficiency of the entire system. In this work, for the sake of simplicity, we assume that the hydrogen present in the retentate stream of the first membrane stage (R1 in **Table 4**) is treated as a process loss ($\dot{m}_{H2,R1}$ = 1.9 kg/h). Furthermore, it is assumed that the total amount of methane contained in the R1 and P2 streams (the permeate stream of the second membrane stage) - amounting to 8.2 kg/h in total ($\dot{m}_{CH_4,R1}$ and $\dot{m}_{CH4,P2}$) - can be fully recovered. Consequently, the overall loss associated with the purification process is approximately the 1.9 kg/h hydrogen stream, resulting in a hydrogen product flow rate of 48.1 kg/h. The complete purification process

outlined by us is not detailed here; its assumptions and results are presented in **Table 4**. The two most important parameters we were interested in were Operational Expenditures (OPEX) and Capital Expenditures (CAPEX) for the entire purification unit, so these are detailed in the table above. Compression work was determined using the following formula:

$$W_{\text{isentrop}} = \frac{\kappa}{\kappa\text{-}1} RT_1 \left[\left(\frac{p_2}{p_1} \right)^{\frac{\kappa\text{-}1}{\kappa}} \text{-}1 \right] \quad (1)$$

$$W = \frac{W_{\text{isentrop}}}{\eta_{\text{isentrop}} \times \eta_{\text{electrical}}} \quad (2)$$

where: κ- heat capacity ratio [-] (for hydrogen it is 1.41); R- specific gas constant [J/kgK];
T_1: gas mixture temperature on the suction side of the compressor [K]
p_1: initial pressure [bar]
p_2: pressure after compression [bar]
η_{isentrop}: isentropic efficiency of the compression [-]
$\eta_{\text{electrical}}$: electric efficiency of the compressor [-]
W_{isentrop}: isentrop specific work of the compression [J/kg]
W: specific work of the compression [J/kg]

When calculating compression requirements, the calculation was simplified by neglecting the effect of methane present in low quantities on the heat capacity ratio (κ). The cooling requirements of the heat exchangers downstream of the compressors were ignored and approximated the OPEX cost of the compressors with the value of the electricity required to drive them.

The CAPEX elements of the membrane separation plant were estimated based on the work of He **[39]** in which compressors and membrane stages correspond to separate items, as shown in **Table 4**. The investment costs of hydrogen compressors were calculated based on the following equation **[5]**:

$$\text{CAPEX} = 36079.54 \times P_{\text{comp}}^{0.6038} \quad (3)$$

where: CAPEX- Capital Expenditure [EUR]; P_{comp}- performance of the compression [kW].

The cost of the membranes is almost negligible compared to that of the compressor **[39]** but an additional cost of 30% for the auxiliary and structural equipment was calculated that maintains the connection between the individual subunits (compressors, membranes) and ensures their operation.

Table 4. The main assumptions and characteristics of the hydrogen purification unit

Compressor unit				
Type	-	-	oil-free reciprocating	
Stages	-	-	2	According to **[37]**
Gas mixture mass flow	$\dot{m}_{\text{H2,pur,in}}$	kg/h	58.2	Assumed mass flow from methane splitting reactor

Compressor unit				
Gas mixture inlet (1st stage) pressure	$T_{1st,in}$	°C	25	Assumed
Gas mixture inlet pressure	p_1	bar	1.8	Our assumed outlet pressure from MS technology
Gas mixture pressure after 1st compression stage	p_2	bar	15	[40]
Gas mixture pressure after 1st heat exchanger	p_3	bar	15	Assuming isobaric heat exchanger
Gas mixture pressure after 1st stage membrane separation (retentate side)	p_4	bar	15	Equals with p_3
Gas mixture pressure after 1st stage membrane separation (permeate side)	p_5	bar	1.1	[40]
Gas mixture pressure after 2nd compression stage	p_6	bar	10	[40]
Gas mixture pressure after 2nd heat exchanger	p_7	bar	10	Assuming isobaric heat exchanger
Gas mixture pressure after 2nd stage membrane separation (permeate side)	p_8	bar	1.1	[40]
Gas mixture pressure after 2nd stage membrane separation (permeate side)	p_9	bar	10	Equals with p_7
Retentate after 1st membrane stage	R1			Fed back to the upstream side of the MS technology
Hydrogen mass flow in R1	$\dot{m}_{H2,R1}$	kg/h	1.9	
Methane mass flow in R1	$\dot{m}_{CH4,R1}$	kg/h	8.0	
Permeate after 1st membrane stage	P1			This stream flows towards the next stage
Hydrogen mass flow in P1	$\dot{m}_{H2,P1}$	kg/h	84.2	
Methane mass flow in P1	$\dot{m}_{CH4,P1}$	kg/h	1.6	
Retentate after 2nd membrane stage	R2			This stream is recycled and fed inlet side of the purification unit
Hydrogen mass flow in R2	$\dot{m}_{H2,R2}$	kg/h	36.1	
Methane mass flow in R2	$\dot{m}_{CH4,R2}$	kg/h	1.4	
Permeate after 2nd membrane stage	P2			This stream is the 99.97 vol% hydrogen product
Hydrogen mass flow in P2	$\dot{m}_{H2,P2}$	kg/h	48.1	
Methane mass flow in P2	$\dot{m}_{CH4,P2}$	kg/h	0.2	
Electricity consumption	P_{comp}	kW	237	Calculated with Equation

Compressor unit				
				(1) and Equation (2)
Specific electricity consumption	e_{comp}	kWh/kg H_2	4.9	Calculated data, within the range of Janusz-Szymańska et al. [41], this specific value refers to 48.1 kg/h pure hydrogen
Isentropic efficiency of the compression	$\eta_{isentrop}$	-	0.85	
Electric efficiency of the compressor	$\eta_{electrical}$	-	0.95	
CAPEX	-	mEUR	1.29	Calculated by Equation (3)
Membranes				
Type	-	-	Well-developed polymer (polyamide) or Carbon Molecular Sieve Membrane (CMSM)	E.g. SEPURAN® or HISELECT®
Selectivity (H_2/CH_4)	α	-	100	[37]
Hydrogen permeance	P_{H2}	GPU	1000	[37]
Total Area	-	m^2	100	[42]
Specific capital investment	-	EUR/m^2	100	[39]
CAPEX	-	mEUR	0.01	
Auxiliary equipment				Pipes, heat exchangers, instrumentation
CAPEX	-	mEUR	0.55	Based on the assumption: 30% of total purification plant
Total CAPEX	**-**	**mEUR**	**1.85**	

Hydrogen Refuelling Station

The hydrogen purification technology is followed by the HRS itself, which includes the hydrogen compressor, the 500 bar pressure buffer tank, and the dispensers. As mentioned earlier, the purpose of the filling station is to supply HDVs with a typical filling pressure of 350 bar (H35 standard), so high-pressure filling (H70, 700 bar) and the associated high-pressure buffer tank are not the subject of our investigation. The suction pressure of the hydrogen compressor is 1.1 bar, and its theoretical pressure on the discharge side is between 350 and 500 bar. The maximum permissible pressure ratio is 2.5 [43], so at least 6 – 7 stages are required to reach the 350 – 500 bar pressure range from the initial 1.1 bar. Franco *et al.* [44] have shown that a higher pressure ratio of up to 5-7 can be achieved, thus requiring fewer compression stages. However, this requires examination of the hydrogen outlet temperature, which must not exceed 150-200 °C due to hydrogen embrittlement problems.

Filling vehicles is regulated by the SAE J2601-2 protocol [45], which also states that the flow after storage and before dispensing does not need to be cooled (Joule-Thomson effect; hydrogen heats up above a certain temperature due to throttling), provided that the protocol is followed, so this was not detailed in this work either. Reddi et al. emphasize that precooling is not necessary when refueling a 350 bar Type III tank [46], which reduces the CAPEX value of the investment.

Table 5. Main assumptions, technology and economy related characteristics of the HRS

Maximal amount of H_2 per day	**kg/day**	**1000**	**Estimated demand**
Utilization rate	%	100	
CAPEX - compressor	mEUR	1.23	Calculated with eq. (1) and eq. (2)
Size of the compressor	kW	344	Calculated with eq. (3)
Type of the compressor	-	oil-free reciprocating	
Minimum stages of the compression	-	6 – 7	
CAPEX - 500 bar storage tank	mEUR	0.8	
Specific CAPEX - 500 bar storage	EUR/kg	800	[43]
Size of the storage	kg	1000	
Dispenser	mEUR	0.03	[43]
Number of dispensers	pcs	1	
Flow rate per dispenser	kg/min	3.6	[45]
Auxiliaries, other costs	mEUR	0.88	Based on the assumption: 30% of total HRS
Total CAPEX	**mEUR**	**2.94**	

Table 5 contains the characteristic values for the HRS and the associated investment costs. In addition to the calculated parameters, the 500 bar hydrogen tank was dimensioned on the basis that it should be able to store enough hydrogen for one day in case the hydrogen supply is interrupted due to maintenance work at the beginning of the process line. Eißler *et al.* arrived at a similar result in their CAPEX estimate, where they estimated the cost of an HRS of the same size at EUR 2.7 million [43]. However, there is a significant difference in the size of the compressors and the number of storage tanks. Eißler et al. examined two types of supply: hydrogen transport via pipeline at a pressure of 80 bar, and road transport, where hydrogen arrives at the HRS at 500 bar and is then transferred to a 200 bar storage tank. This means that in our case, the compressor will have a higher capacity and higher power consumption, as it will need to compress from 1.1 bar to 500 bar. Another difference is that our layout does not include a 200 bar buffer tank, which reduces the total CAPEX of the HRS.

RESULTS AND DISCUSSIONS

Carbon Intensity

In addition to techno-economic calculations, this study also examined the GHG intensities of individual fuels, as this aspect is often overlooked when assessing hydrogen mobility, with analyses frequently focusing solely on economic opportunities. The environmental impact of methane splitting technology was examined by Bulfaro *et al.* [10] in a review article, where they analyzed the studies published to date based on the type of technology (conventional gas, molten media, and plasma) and the types of raw materials and environmental impact assessments. However, no study was mentioned that took biomethane into account as a raw material, and competing methane splitting technologies were not or only minimally presented. As a result, a simplified calculation was performed for ten cases, which are presented in **Table 6** along with considerations and assumptions.

In the case of grey hydrogen, the calculated carbon footprint includes the upstream and midstream emissions associated with natural gas, that is, emissions from exploration through to the point of use (hydrogen production). In an SMR plant, greenhouse gas emissions occur at several stages, released into the environment in the form of carbon dioxide and methane. Carbon dioxide originates from the chemical reaction and from the combustion of fuel, while methane emissions are primarily attributable to fugitive sources [47], [48]. Although the volumetric quantity of methane emissions is almost negligible compared to carbon dioxide, its GWP100 (Global Warming Potential over 100 years) is approximately 30 times higher. The literature typically reports lower values for grey hydrogen, in the range of 11–14 kg CO_2 eq./kg H_2, which, however, do not account for methane emissions [9]. For this hydrogen pathway, the environmental impacts associated with infrastructure development (e.g., hydrogen production facilities) were likewise not included in the calculation.

For turquoise hydrogen, the simplified carbon footprint assessment focused on the emission factors of the input materials. The emission intensity of electricity was determined based on ENTSO-E data (full life cycle assessment) [49], while the natural gas values were taken from the literature referenced above, incorporating upstream and logistical emissions [48]. The GHG emissions of geothermal electricity also reflect a full life cycle perspective, based on NREL research [50]. The emission factor for biogas was determined according to the following logic. Under the guidelines of the European Union [51] biomethane qualifies as a renewable fuel if it achieves an 80% emission reduction. This requirement is based on the fossil comparator value of 94 gCO_2 eq./MJ, implying that biomethane may have a maximum of 18.8 gCO_2 eq./MJ on a full life cycle basis. This upper limit is reflected in Case 5 and Case 6. When manure is used as the feedstock for biomethane production, “negative” emissions may be achieved; in this case, the IEA study served as the basis, and the median number of the two extreme values was applied. Here as well, emissions refer to the full life cycle (feedstock collection, technological processes, post-treatment, purification, etc.). For this hydrogen pathway, the environmental impacts associated with infrastructure development (e.g., methane-splitting facilities) were likewise not included in the calculation. The detailed methods utilized for each scenario are described below.”

Table 6. The scenarios used in the GHG emission analysis for different fuels

Fuel	Assumptions
Case1: Diesel	Calculated based on EU REDIII fossil comparator (94 gCO_2e/MJ)
Case2: Grey hydrogen	Calculated based on life cycle assessment of natural gas supply and the operational emission of an average SMR

Fuel	Assumptions
	□ GHG emission from SMR construction is excluded from this work
Case3: Turquoise hydrogen – NG&grid	□ Calculated based on life cycle assessment of natural gas supply and life cycle emission of the hungarian national electricity grid (2024 fact data) □ GHG emission from construction of Methane Splitting unit is excluded from this work
Case4: Turquoise hydrogen – NG&GEO	□ Calculated based on life cycle assessment of natural gas supply and life cycle emission of an average geothermal power plant (NREL data) □ GHG emission from construction of Methane Splitting unit is excluded from this work
Case5: Turquoise hydrogen – BIO&grid	□ Calculated based on life cycle assessment of biomethane supply (IEA data) and life cycle emission of the hungarian national electricity grid (2024 fact data) □ GHG emission from construction of Methane Splitting unit is excluded from this work
Case6: Turquoise hydrogen – BIO&GEO	□ Calculated based on life cycle assessment of biomethane supply (IEA data) and life cycle emission of an average geothermal power plant (NREL data) □ GHG emission from construction of Methane Splitting unit is excluded from this work
Case7: Turquoise hydrogen – BIO (manure)&grid	□ Same assumptions as in case 5, but the source of the biomethane is from manure, resulting much lower GHG intensity
Case8: Turquoise hydrogen – BIO (manure)&GEO	□ Same assumptions as in case 6, but the source of the biomethane is from manure, resulting much lower GHG intensity
Case9: Electrolysis – grid	□ Calculated based on life cycle emission of the hungarian national electricity grid (2024 fact data) □ The specific electricity consumption of the electrolysis assumed 60 kWh/kg hydrogen □ Excluded from the current scope: o GHG emission from construction of electrolyzer unit o GHG emission from water supply
Case10: Electrolysis - GEO	□ Same assumptions as in case 10, but the source of the electricity is from an average geothermal power plant (NREL data)

The emission values were calculated for a distance of 100 km (most often referred to in the literature as "well-to-wheel" GHG intensity), so that, taking certain conditions into account (see **Table 6**) they can be compared and conclusions can be drawn from them. Diesel-powered heavy-duty vehicles were chosen as the basis for comparison with hydrogen-powered vehicles, as these vehicles still dominate transportation today. The GHG emissions of diesel HDVs per 100 km are 102 $kgCO_2$ eq., which is 45% higher than the most pessimistic turquoise hydrogen option (Case 5: Turquoise hydrogen – BIO&grid), but is the same as the equally pessimistic electrolysis scenario (Case 9: Electrolysis – grid), which was determined based on the GHG emissions of energy purchased from the Hungarian electricity grid in 2024 (242.7 gCO_2 eq./kWh, ENTSOE data). Conversely, this also means that the breakeven GHG emissions of the electricity used for electrolysis are the aforementioned 242.7 gCO_2 eq./kWh, taking into account the defined criteria. In other words, above this value, the GHG emissions of electrolytic hydrogen are higher than the fuel emissions of

diesel-powered HDVs. Water splitting (or electrolysis) technology is sensitive to electricity parameters (such as GHG emissions or price), so when connected to a low GHG intensity energy source, the fuel footprint also drops significantly, as shown in **Figure 4**. Hydrogen produced by electrolysis connected to a geothermal power plant [50] and then used in a fuel cell can reach a value of up to 15 $kgCO_2$ eq./100km, which is roughly 7 times less GHG emissions than its diesel competitor.

While GHG emissions from electrolytic hydrogen depend almost exclusively on the electricity used, in the case of turquoise hydrogen, the origin of the methane used as a raw material can also be crucial in this regard. In the cases marked NG (Case 3 and Case 4 in **Table 6**), the source of methane is natural gas, whose GHG intensity for transport to the point of use is 17.2 gCO_2 eq./MJ according to JRC Technical Reports [48]. Case5 and Case6, in which the abbreviation BIO stands for biomethane feedstock, do not differ significantly from these cases in terms of GHG emissions. The International Energy Agency (IEA) also examined the GHG emissions of biomethane over its entire life cycle in 2025 [12], which yielded a wide range of results depending on the raw material (manure, maize whole crop, and biowaste raw materials). Due to this phenomenon, calculations were based on the EU Renewable Energy Directive III (RED III) [51], which stipulates a mandatory 80% reduction in GHG emissions from biomass-based biofuels from 1 January 2026. This means that 20% of the fossil comparator value of 94 gCO_2 eq./MJ can be calculated, i.e. 18.6 gCO_2 eq./MJ, which is almost the median value of the emissions of biogas plants examined by the IEA. Both of the above cases were evaluated with different types of electricity supplies; as in case of electrolysis; using data from the Hungarian electricity grid and the average values typical of geothermal power plants (Case 3-Case 6). Since there is no significant difference between the GHG emissions of methane sources (17.2 gCO_2 eq./MJ for natural gas and 18.6 gCO_2 eq./MJ for biomethane), their emissions projected over 100 km are very similar. It is worth noting again that this phenomenon is due to the fact that different biomethane sources have very different emission values, and the value calculated from the fossil comparator is a maximum permissible value for newly installed biomethane plants. However, the decisive difference between the scenarios is the source of electricity, since if energy purchased from the Hungarian grid is used, the emissions are 68 $kgCO_2$ eq./100 km in the case of natural gas (Case 3) while in the case of biomethane (Case 5) it is 70 $kgCO_2$ eq./100 km, which is 33.3% and 31.4% lower than in the case of diesel fuel and electrolytic hydrogen (Case 9), respectively. By using renewable energy, in this case geothermal electricity, emissions can be significantly reduced to 31 and 33 $kgCO_2$ eq./100 km (Case 4 and Case 6), representing reductions of 69.6% and 67.6%, respectively, which are still roughly twice as high as in the case of hydrogen produced by electrolysis using only renewable electricity (Case 10, 15 kg CO_2 eq./100 km). In general, Cases 3 – 6 can achieve significant GHG emission reductions in transportation compared to the diesel version, especially if the electricity is sourced from renewable sources (e.g., geothermal) and compared to electrolytic hydrogen, which cannot be considered green (Case 9), it is also much more favorable in terms of emissions.

The cases include two cases with negative GHG emissions over the entire life cycle (Case 7 and Case 8), which are special but by no means insignificant. In the cases examined, the source of biogas, and thus biomethane, is animal manure and other animal-derived waste, which has an average GHG emission of −45 gCO_2e/MJ, as this type of biomass would cause very significant methane emissions due to the oxygen in the air [12]. If biomethane is produced from this animal-derived organic material, the resulting GHG emissions of the biomethane itself are negative, or possibly slightly positive, in the range of (−)95−5 g CO_2e/MJ. For simplicity, the arithmetic mean of these values was used in the emission calculations. The results show that in both Case 7 and Case 8, even electricity supplies with different emission values do not turn the GHG emissions of turquoise hydrogen positive (−19 and −56 kg CO_2 eq./100 km). It is worth noting that these are the only cases in which

carbon-negative hydrogen can currently be produced. Obviously, this requires the negative emission value of the raw material biomethane, but with other technologies we encounter technical and thermodynamic obstacles if we want to achieve a negative or near-carbon-neutral zone.

Overall, it can be stated that the general biomethane emission approach used in the turquoise hydrogen emission assessment results in a wide range, with the emission values obtained falling between the extreme values of alternative hydrogen production technologies and diesel fuel. Grey hydrogen is the fuel with the highest GHG intensity, similar to the values for diesel and electrolytic hydrogen (Case 9). Green hydrogen (Case 10) borders the range of turquoise hydrogen calculated with average biomethane emissions from below. If the raw material for biomethane is sourced from organic materials of animal origin, we obtain carbon-negative hydrogen, which generates an emission deficit rather than GHG emissions throughout the entire process, from biomethane production through hydrogen production to fuel consumption. All of the data used for GHG emission calculation can be found in ANNEX.

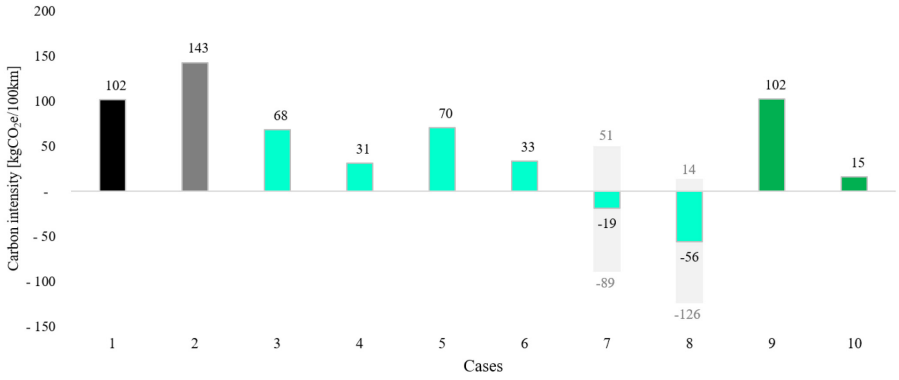

Figure 4. Results of the GHG assessment of the ten different scenarios

Economic Analysis

The GHG emissions analysis presented above shows that turquoise hydrogen has significantly lower emissions per 100 km traveled than diesel, gray hydrogen, and, in some extreme cases, electrolytic hydrogen. In certain scenarios, the total GHG emissions of a given biomethane feedstock may be negative. The environmental impact is an extremely important factor, but the driving force behind the large-scale adoption of individual technologies is primarily a question of economics. Of course, decision-makers can promote the speed and extent of deployment through various support systems, but if a given solution is far from competitive due to some techno-economic barrier, investors may become uncertain and back away from using low-carbon or green technologies. This phenomenon can be seen in the example of green hydrogen and electrolysers, as presented by Jesse *et al.* [52].

Investigated scenarios. During the analysis, three different scenarios were examined in which the technical, support, and market aspects were varied on the production side, while studying the extent of support on the consumption side using different extreme values. The cases were designed to include an optimistic, a moderately optimistic, and a pessimistic outcome (Table 7). The "Rapid expansion" optimistic scenario sets the goal of ensuring that the technical solution outlined in the case study can be quickly implemented as a so-called "blueprint" and, under certain conditions, can be applied simultaneously in several locations, at busy intersections, but ideally in logistics centers or possibly at the depots of vehicles involved in public transport. It should be noted that the case study is based on biomethane produced at

the Szarvas biogas plant, but if the key conditions are met, the technology can be transferred to other locations. In terms of raw materials, in this case, natural gas will be used from the starting year (2028) until 2038, i.e. for the first 10 years, which is much cheaper than biomethane, thus keeping the cost of hydrogen lower over a 20-year period. It is important to acknowledge that a natural-gas-based technology does not fully ensure security of supply, as Hungary relies almost entirely on imports to meet its natural gas demand. However, within a clearly defined transitional period, it may still serve as a viable alternative in the context of sustainability and green mobility (this fact is supported by the results obtained in the previous section), supporting the early market uptake and adoption of the technology. In this case, the CAPEX support for the technology investor is 50%, and carbon black is sold at a price of 1100 EUR/t, which, according to Dagle *et al.* [26] is considered a moderate specific price and appears in all three scenarios. At the price level considered (~1100 EUR/t), the most commonly traded products are the smaller-particle grades (11 –30 nm), such as N100 – N300. However, there are periods when softer grades (N500 – N700) also appear on the spot market at comparable price levels [53]. As a conservative assumption – and to ensure that the analytical focus remains on hydrogen – using the harder N220 and N330 grades provides a reasonable and robust approximation under current market conditions. Customer support consists of two parts: a one-time CAPEX subsidy for the purchase of a Fuel Cell Electric Vehicle (FCEV) worth EUR 100,000, and an OPEX subsidy worth 1 EUR/kg for the entire life cycle (20 years). A detailed analysis of the consumer side can be found in the following section.

"Moderate progress" involves a smaller-scale support scheme, in which the natural gas utilization period is also shorter, at only four years. In this case, the production and the demand sides are less artificially accelerated. The "Hard-to-implement" case shows the current economic indicators of such decentralized low (or negative) GHG emission hydrogen mobility without subsidies. Neither the producer nor the consumer side benefits from subsidies; such investments can only be market-based. The results of the scenarios are presented in the following sections.

Table 7. Investigated scenarios during the economic analysis

		"Rapid expansion"	**"Moderate progress"**	**"Hard-to-implement"**
Description		Strong government support for the prompt expansion of the hydrogen mobility; Slow transition from natural gas to biomethane; Reliable market for CB	Moderate government support for the slow expansion of the hydrogen mobility; Relatively quick transition from natural gas to biomethane; Reliable market for CB	Not existing government support; Start with biomethane instantly; Reliable market for CB
Methane source	-	NG (2028-2038) BIO (2038-2048)	NG (2028-2032) BIO (2032-2048)	BIO
Electricity source	-	direct renewable (geotherm)	direct renewable (geotherm)	direct renewable (geotherm)
Carbon black price	EUR/t	1100	1100	1100
CAPEX subsidy for HRS Investor&Operator	%	50	25	0
Subsidy scheme for Customer	-	CAPEX: 100 000 EUR/truck OPEX: 1 EUR/kg H_2/truck	CAPEX: 50 000 EUR/truck OPEX: 1 EUR/kg H_2/truck	No subsidy

Breakeven cost calculation for FCEV Customer. In order to evaluate our entire technology range more accurately, we need a reference point, which in this case is the diesel-powered HDV. **Table 8** contains the data and assumptions required for the comparison. The economic calculation was made with the aim of finding the specific hydrogen cost at which it becomes worthwhile for a company to purchase and operate hydrogen-based FCEV trucks or buses, so this calculation is essentially interpretable from their point of view (Customer).

Table 8. Utilized data during the investigation of breakeven hydrogen cost from the FCEV Customer point of view

		FCEV	**Diesel**
Annual covered distance by one truck	km	100 000	100 000
Hydrogen consumption	kg/100 km	7	-
Diesel consumption	l/100 km	-	30
Yearly hydrogen consumption	kg	7 000	-
Yearly diesel consumption	l	-	30 000
Cost of diesel (fixed)	EUR/l	-	1.6
Annual diesel cost per truck (OPEX)	EUR/truck/year	-	48 000
CAPEX of one truck	EUR/truck	500 000	150 000
Country Risk Premium	CRP	%	0.5
Weighted average cost of capital	WACC	%	6
"n"th year after the investigation date (2025)	n	-	-
Free cash flow to the firm	FCFF	EUR	time-varying

Using eq. (4), eq. (5) and eq. (6), the annual expenditure was calculated on hydrogen fuel at which the net present value (NPV) of an FCEV investment is equal to zero. The calculations are performed for a period of 20 years, with a CRP of 0.5% and a WACC of 6%. The scenarios outlined in **Table 7** have different subsidy schemes, so the calculation must be performed for each of them. **Table 9** shows the results for each case, which serve as important inputs for the economic calculation described below.

$$\mathrm{FCFF}(n) = \mathrm{CAPEX}_{\mathrm{diesel}} - \mathrm{CAPEX}_{\mathrm{FCEV}} + \mathrm{OPEX}_{\mathrm{diesel}} - \mathrm{OPEX}_{\mathrm{FCEV}} + \mathrm{CAPEX}_{\mathrm{sub}} + \mathrm{OPEX}_{\mathrm{sub}} \quad (4)$$

$$\mathrm{d}f(n) = \frac{1}{1 + (\mathrm{WACC} + \mathrm{CRP})^{n+0.5}} \quad (5)$$

$$\mathrm{NPV} = \sum_{n=1}^{20} \mathrm{d}f(n) \times \mathrm{FCFF}(n) \quad (6)$$

Table 9. Results of the breakeven hydrogen cost analysis

Breakeven H_2 cost for the Customer (EUR/kg H_2)					
"Rapid expansion"	CAPEX subsidy	$CAPEX_{sub}$	EUR	100 000	4.81
	OPEX subsidy	$OPEX_{sub}$	EUR/kg H_2	1	
"Moderate progress"	CAPEX subsidy	$CAPEX_{sub}$	EUR	50 000	4.20
	OPEX subsidy	$OPEX_{sub}$	EUR/kg H_2	1	
"Hard-to-implement"	CAPEX subsidy	$CAPEX_{sub}$	EUR	0	2.60
	OPEX subsidy	$OPEX_{sub}$	EUR/kg H_2	0	

Economic analysis of the whole plant. The economic analyses were prepared based on the scenarios mentioned above, the details of which are shown in **Table 10**. It is worth mentioning that, based on the data in **Table 9**, an HRS with a capacity of 1 t/d could theoretically serve 52 FCEV trucks or buses annually. This number may change slightly if charging times and schemes are also taken into account, but these are not examined within the scope of this work.

The economic analysis has two objectives: on the one hand, it aims to determine the unit price of hydrogen at which the NPV of HRS Investor&Operator is 0, or, in other words, the selling price of hydrogen to the customer at which the investment will pay for itself at the end of 20 years. On the other hand, it provides useful information on the LCOH value determined for the entire investment period of hydrogen and its breakdown into components. The difference between the "Hydrogen sales price" and the LCOH will also be analyzed later.

Table 10. Utilized data during the Economic analysis for each scenario

		"Rapid expansion"	**"Moderate progress"**	**"Hard-to-implement"**
Economy				
Amortization	%		5	
WACC	%		6	
CRP	%		0.5	
Inflation	%		2	
Corporate Income Tax (CIT)	%		9	
HUF/EUR FX	-		400	
USD/EUR FX	-		0.9	
Energy and other cost premises				
Geothermal electricity cost	EUR/MWh	Considering IRENA 2010-2024 dataset, with linear extrapolation until 2048 [23]. Defined as Levelised Cost of Electricity (LCOE)		
Biomethane cost	EUR/MWh	Currently the biomethane cost is 71 EUR/MWh, which will decrease by 13% by 2050 [12]		
Natural gas cost	EUR/MWh	Starting 30 EUR/MWh in 2025 and adjusted with the inflation until 2048		
Estimated Full Time Employee (FTE) cost	EUR/FTE/year	15 000		
Business Case details				
Hydrogen production	t/year	365		

		"Rapid expansion"	"Moderate progress"	"Hard-to-implement"
Nominal hydrogen capacity of plant	t/year		421	
Utilization rate	%		86.6	
	h/year		7588	
Hydrogen sales volume to Customer(s)	t/year		365	
Produced CB	t/year		1095	
Feedstock NG/biomethane	t/year		1518	
Feedstock electricity (process)	MWh/year		3794	
CB sales price [26]	EUR/t	1100	1100	1100
Feedstock NG/biomethane cost	mEUR/year	Calculated by NG/biomethane premises and its amount		
Feedstock electricity (process) cost	mEUR/year	Calculated by Geothermal electricity premises and electricity need		
OPEX – personell cost	mEUR/year	0.03 (2 FTE)		
OPEX – maintenance cost	mEUR/year	0.27 (3% of total CAPEX)		
OPEX – Electricity (MS-auxiliaries, purification, compression with waste heat recovery)	MWh/year		5092	
	mEUR/year	Calculated by Geothermal electricity premises and electricity need		
CAPEX - MS	EUR/kW		8000 [9]	
CAPEX - MS	mEUR		4.00	
CAPEX – ORC waste heat	mEUR		0.33 [28]	
CAPEX – Purification system	mEUR		1.85	
CAPEX - HRS	mEUR		2.94	
Total CAPEX	mEUR		9.12	
CAPEX subsidy	%	50	25	0
Adjusted CAPEX	mEUR	4.56	6.84	9.12

The analysis is based on a classic revenue-expense calculation, in which each item has been identified. To determine the NPV, similar to the FCEV breakeven hydrogen cost, eq. (4), eq. (5) and eq. (6) were used. The LCOH and hydrogen sales price were determined by finding the values corresponding to NPV=0 in each model. The LCOH is a figure characteristic of a given technology or technology series for an entire operating period, which shows the average discounted cost of producing one kilogram of hydrogen during the period under review. This differs from the hydrogen sales price in that, while according to our calculations this value is constant for the entire operating period, the annual costs per kilogram of hydrogen vary and are adjusted by the discount factor. This is why the hydrogen sales price is always higher than the LCOH.

Figure 5 shows the LCOH and hydrogen sales price values for each scenario, indicating the individual components of LCOH in each case. The scenarios examined have in common the costs incurred for electricity for the process (0.57 EUR/kg), electricity for auxiliary equipments, hydrogen purification, compression (0.77 EUR/kg) and labor (personnel) plus the maintenance cost (0.83 EUR/kg). These scenarios are also identical in terms of CB sales, since, as discussed earlier, the unit selling price of CB was set at EUR 1100/t in all cases.

The main difference between the scenarios is the cost of natural gas/biomethane used as feedstock. **Figure 5** shows that in case a, ("Rapid expansion"), the methane required for the technology would be covered in the form of natural gas until 2038, i.e. for half of the total operating period, which would mean a significant cost reduction compared to case c, ("Hard-to-implement") shown in the figure, where biomethane would have to be purchased throughout the entire period. This results in an additional cost of 1.26 EUR/kg for this item alone. In case b, ("Moderate progress"), the share of natural gas/biomethane projected for the entire operating period is 3.24 EUR/kg, which assumes that the transition from natural gas to biomethane will take place after 2032. Although not significant, there are also differences between the individual CAPEX items in the cases, which are 0.63 ("Rapid expansion"), 0.93 ("Moderate progress") and 1.24 EUR/kg ("Hard-to-implement").

For each examined case, the LCOH and hydrogen sales price values are shown in **Figure 5** and in **Table 11**.

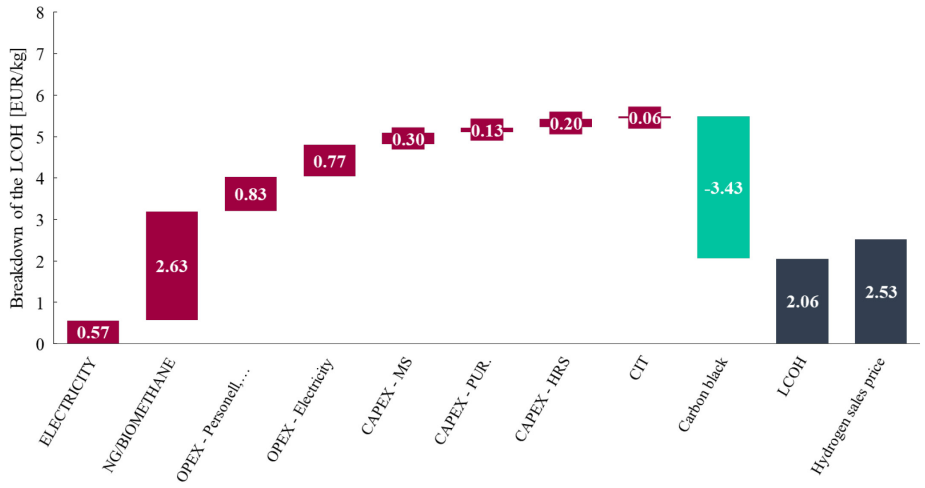

(a)

(b)

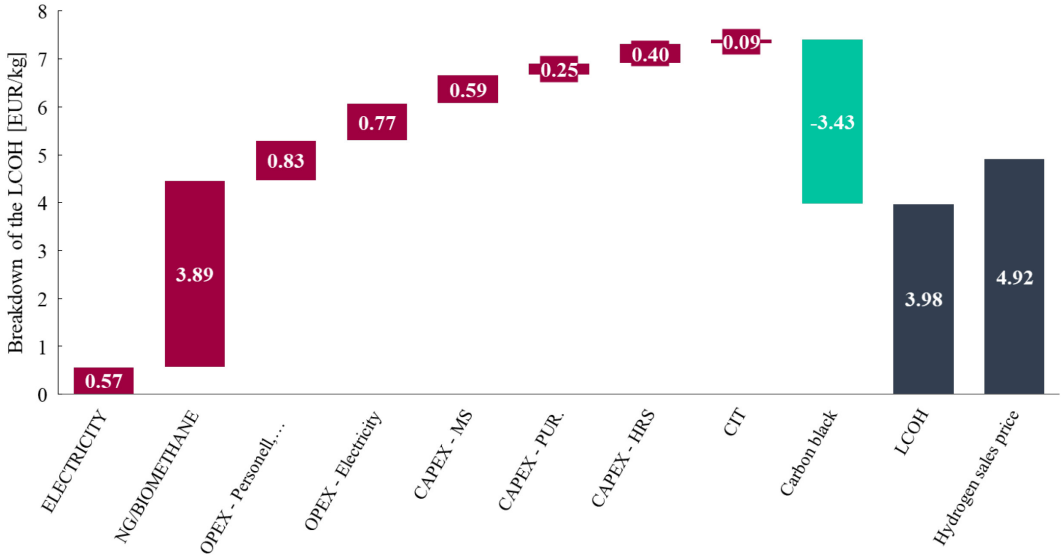

(c)

Figure 5. The Economy results of the three investigated scenarios including the LCOH breakdown and the hydrogen sales price to the customer:
(a) Rapid expansion; (b) Moderate progress; (c) Hard-to-implement

Table 11 shows the results of the economic analysis in terms of LCOH and hydrogen sales price values for the three scenarios. In the "Rapid expansion" case, the LCOH value is 2.06 EUR/kg, and the hydrogen sales price, at which the customer purchases the fuel for 20 years, is 2.53 EUR/kg. Consumer support is most significant in this scenario, which is why the "H_2 Breakeven cost for Customers" is the highest, at 4.81 EUR/kg H_2. This means that if the price of hydrogen is lower than this, investing in FCEVs is positive and economically justified. As mentioned earlier, the production side is able to sell hydrogen at a price of at least 2.53 EUR/kg, therefore, the difference between the two, or the profit of HRS Investor&Operator (if the H_2 sales price to Customer rises to 4.81 EUR/kg), improves the Customer's return. In the latter case, the Customer can actually purchase hydrogen at a price of 2.53 EUR/kg. **Table 11** shows the former case, where HRS Investor&Operator realizes the profit from the price difference. This version represents a NPV of 7.19 million EUR with an IRR of 29.9%, which may be a sufficient incentive for the implementation of such a project.

In the "Moderate progress" scenario, both the LCOH (2.99 EUR/kg) and the H_2 sales price (3.70 EUR/kg) are higher than in the previous case. This is due, on the one hand, to lower CAPEX support (25% instead of 50%) and, on the other hand, to the shorter period of natural gas use (only until 2032 instead of 2038). However, the "H_2 breakeven cost" for the customer is lower (4.20 EUR/kg), also due to the lower subsidy volume (CAPEX subsidy reduced from EUR 100,000 to EUR 50,000). Despite this, the difference between the "H_2 breakeven cost" and the "H_2 sales price" remained, although its value decreased, and if this difference is also realized by HRS Investor&Customer, the NPV is 1.58 million EUR, with an IRR of 10.5%, which is much less of an incentive to invest than the aforementioned "Rapid extension" scenario.

Table 11. The most important outcomes from Economic analysis

		"Rapid expansion"	"Moderate progress"	"Hard-to-implement"
LCOH (2028-2048)	EUR/kg	2.06	2.99	3.98
H_2 sales price to Customer (fix value) (2028-2048)	EUR/kg	2.53	3.70	4.92
H_2 Breakeven cost for Customers	EUR/kg	4.81	4.20	2.60
NPV†	mEUR	7.19	1.58	-
IRR‡	%	29.9	10.5	-

In the "Hard-to-implement" case, the LCOH value is 3.98 EUR/kg, with a sales price of 4.92 EUR/kg. In this case, there is no subsidy system on either the producer or consumer side, so we can only calculate based on the material and energy balance. The customer's "H_2 breakeven cost" is 2.60 EUR/kg, which is a very low value due to the lack of the aforementioned subsidies. In this case, the producer side is no longer able to offer the customer a competitive price that would allow them to recoup their FCEV investment. For this reason, the NPV and IRR values are not shown. If we examine the circumstances of our case study, without subsidies and all other incentives, this case is the closest to it, as the solution can be interpreted purely on a competitive market basis.

It is worth noting that the support schemes for the producer and consumer sides outlined in each scenario can be combined arbitrarily, for example, the producer side of the “Rapid expansion” (natural gas until 2038, 50% CAPEX support) can be linked to the “Hard-to-implement” consumer side, when there is no incentive support for either CAPEX or OPEX. In relation to the specific example, the 2.53 EUR/kg supply, producer side price can just satisfy the 2.60 EUR/kg “Breakeven cost”.

One should keep in mind that the prices of some “parts” can be reduced under special circumstances. For example, the geothermal electricity cost can be much lower when the geothermal power plant is installed on an existing, underused geothermal well [54]; in this way, financial viability can be improved, although finding a proper location for the on-site hydrogen refuelling station could be more challenging.

To demonstrate the robustness of the results and to highlight the relative importance of the key model parameters, a sensitivity analysis was performed for one selected scenario. In the case of the Rapid Expansion scenario, the analysis focused on the resulting LCOH values, examining the influence of the CAPEX subsidy level, the CB sales price, and the annual hydrogen sales volume (see Table 12).

† if the difference belongs to the HRS Investor&Operator
‡ if the difference belongs to the HRS Investor&Operator

Table 12. Sensitivity analysis of scenario "Rapid expansion"

CB sales price [EUR/t] \ CAPEX subsidy of MS-HRS plant [%]	10%	30%	40%	50%	60%	70%	90%
800	3.43	3.19	3.06	2.94	2.83	2.71	2.47
900	3.12	2.89	2.77	2.65	2.53	2.42	2.18
1000	2.83	2.59	2.47	2.36	2.24	2.12	1.89
1100	2.53	2.30	2.18	**2.06**	1.95	1.83	1.59
1200	2.24	2.01	1.89	1.77	1.65	1.54	1.31
1300	1.95	1.71	1.60	1.48	1.37	1.25	1.02
1400	1.65	1.42	1.31	1.20	1.08	0.97	0.74

CB sales price [EUR/t] \ Hydrogen sales volume [t/year]	146	183	219	256	292	329	365
800	7.31	5.85	4.88	4.19	3.67	3.26	2.94
900	6.54	5.24	4.37	3.75	3.28	2.93	2.65
1000	5.77	4.62	3.85	3.31	2.91	2.60	2.36
1100	4.99	4.00	3.34	2.88	2.54	2.28	**2.06**
1200	4.22	3.39	2.85	2.46	2.18	1.95	1.77
1300	3.47	2.80	2.36	2.05	1.81	1.62	1.48
1400	2.73	2.22	1.87	1.63	1.44	1.30	1.20

In the sensitivity analysis examining the effects of CAPEX subsidy and the CB sales price, it can be concluded that the LCOH is relatively sensitive to both parameters. In the table, the LCOH value of 2.06 EUR/kg − corresponding to the base case − is highlighted, which is obtained at a 50% CAPEX subsidy and a CB sales price of 1100 EUR/t. At this CB price level, increasing the CAPEX subsidy further can reduce the LCOH to as low as 1.59 EUR/kg, whereas moving in the opposite direction, a subsidy intensity of only 10% increases the LCOH to 2.53 EUR/kg (a 22.8% increase). The influence of the CB sales price is also substantial: it is evident that at CB prices of 1300 – 1400 EUR/t, hydrogen becomes clearly competitive with the lowest-cost grey hydrogen. However, at lower CB price levels, the resulting LCOH remains far from the cost range of electrolytic hydrogen.

When examining the effect of hydrogen sales on the LCOH, what is essentially being assessed is the extent to which the share of capital-related costs within the LCOH can be reduced. In other words, these are the cost components that do not depend on production capacity and can be lowered by producing and selling larger volumes of hydrogen, provided that a stable and predictable market demand is available. It is worth noting that if at least 90% of the produced hydrogen is sold (>329 t/year), the LCOH remains below approximately 3 EUR/kg even at low CB sales prices, which can still be considered competitive. The advantages and overall effectiveness of the technology outlined in this work diminish substantially when the utilisation rate of the HRS falls to 50% or below. Such a low utilisation level would indicate the absence of a stable demand side, implying that a smaller production plant and refuelling station configuration would have been more appropriate. This analysis partly supports the conclusion that one of the most critical considerations in sizing a HRS is the demand side. A robust and predictable hydrogen demand is essential for developing an appropriate production and refuelling infrastructure strategy.

CONCLUSION

This biomethane-based solution can be a promising alternative for countries with existing high-capacity biogas station network as well as it can be a future solution for countries where agricultural "waste" can be used to produce good quality biogas in the future. This work proves that, in addition to technological feasibility, the concept could offer low-carbon (or even carbon-negative) hydrogen at realistically affordable price which could compete with fossil fuels within certain limits.

- Three scenarios were investigated which differ in the feedstock utilization (biomethane and natural gas), CAPEX subsidy for HRS Investor&Operator and CAPEX&OPEX subsidy for the Investor of FCEV trucks. "Rapid expansion" case could offer hydrogen at 2.53 EUR/kg price which is really competitive even without CAPEX and OPEX subsidy for the Investor of FCEVs (2.60 EUR/kg). "Moderate progress" case provides hydrogen at higher price (3.70 EUR/kg), although this remains affordable if Investor of the FCEVs could apply for subsidies. "Hard-to-implement" case operates purely on market basis, no subsidy scheme occur in this scenario. Nevertheless the LCOH and the sales price of this case (3.98 and 4.92 EUR/kg) remain competitive against the onsite electrolytic hydrogen based on Perna *et al.* [5], where the LCOH of the onsite electrolysis system was calculated 7.92 EUR/kg, and the literatures data for this design are shown a range 5.97-15.7 EUR/kg.
- There are several constrain to apply this whole method (on-site hydrogen production from biomethane, powered by geothermal power, sources located along main motorways), but for example in the Pannonian Basin, the number and distribution of geothermal sources as well as the capacity of the area to produce raw material for biogas enables neighbouring countries (like Croatia, Slovenia, Austria, Slovakia, Romania, Serbia and Hungary) to choose this solution, at least in some areas

ACKNOWLEDGMENT

Project no. RRF-2.3.1-21-2022-00009, titled National Laboratory for Renewable Energy has been implemented with the support provided by the Recovery and Resilience Facility of the European Union within the framework of Programme Széchenyi Plan Plus. Part of the research research was funded by the Sustainable Development and Technologies National Programme of the Hungarian Academy of Sciences (FFT NP FTA). Project no. KDP-IKT-2023-900-I1-00000957/0000003 has been implemented with the support provided by the Ministry of Culture and Innovation of Hungary from the National Research, Development and Innovation Fund, financed under the KDP-2023 funding scheme.

NOMENCLATURE

Acronyms/Abbreviations/Chemical Formula

BIO	biomethane
BIO(manure)	biomethane from manure source
CAPEX	capital expenditures
CB	carbon black
CMSM	carbon molecule sieve membrane
CO_2	carbon-dioxide
CHP	combined heat and power
CIT	corporate income tax
CRP	country risk premium
GEO	electricity from the geothermal power plant
grid	electricity from the national grid

FX	foreign exchange
FCFF	free cash flow to the firm
FCEV	fuel cell electric vehicle
FTE	full time employee
GHG	greenhouse gases
GWP	Global Warming Potential over 100 years
HDV	heavy duty vehicle
H_2	hydrogen
IEA	International Energy Agency
LCOE	levelised cost of electricity
LCOH	levelised cost of hydrogen
LHV	lower heating value
CH_4	methane
MS	methane splitting
mEUR	million euros
NG	natural gas
Nm^3	normal cubic meter
NPV	net present value
OPEX	operational expenditures
PSA	pressure swing absorption
RED III	Renewable Energy Directive III
ROI	Return on Investment
ORC	organic Rankine Cycle
TRL	technology readiness level
TEN-T	Trans-European Transport Network
WACC	weighted average cost of capital

Equation Variables

Equation (1)		
κ	heat capacity ratio	-
R	specific gas constant	J/kgK
T_1	gas mixture temperature on the suction side of the compressor	K
p_1	initial pressure	bar
p_1	pressure after compression	bar
$W_{isentrop}$	isentrop specific work of the compression	J/kg
Equation (2)		
$\eta_{isentrop}$	isentropic efficiency of the compression	-
$\eta_{electrical}$	electric efficiency of the compressor	-
W	specific work of the compression	J/kg
Equation (3)		
CAPEX	capital expenditure	EUR
P_{comp}	performance of the compression	kW
Equation (4)		
FCFF	free cash flow to the firm	EUR
$CAPEX_{diesel}$	capital expenditure of the diesel HDV	EUR
$CAPEX_{FCEV}$	capital expenditure of the FCEV HDV	EUR
$OPEX_{diesel}$	operational expenditure of the diesel HDV	EUR

$OPEX_{FCEV}$	operational expenditure of the FCEV HDV	EUR
$CAPEX_{sub}$	capital expenditure subsidy for the Customer	EUR
$OPEX_{sub}$	operational expenditure subsidy for the Customer	EUR
Equation (5)		
CRP	Country Risk Premium	%
WACC	Weighted average cost of capital	%
df	discount factor	-
Equation (6)		
NPV	net present value	EUR

REFERENCES

1. Deloitte-Ballard white paper on fuel cells for fueling future mobility, Fuel Cells Bulletin, Vol. 2020, No. 2, 12, 2020, https://doi.org/10.1016/S1464-2859(20)30076-6.
2. G. Trencher, Strategies to accelerate the production and diffusion of fuel cell electric vehicles: Experiences from California, *Energy Reports*, Vol. 6, pp 2503–2519, 2020, https://doi.org/10.1016/j.egyr.2020.09.008.
3. M. A. Alreshidi et al., Hydrogen in transport: a review of opportunities, challenges, and sustainability concerns, *RSC Adv.*, Vol. 15, No. 29, pp 23874–23909, 2025, https://doi.org/10.1039/D5RA02918J.
4. K. Kummer and A. R. Imre, Supply of the hydrogen refuelling stations in the Hungarian part of the Trans-European Transport Network – comparison of the methane splitting and water electrolysis, *Int. J. Hydrogen Energy*, Vol. 186, 152084, 2025, https://doi.org/10.1016/j.ijhydene.2025.152084.
5. A. Perna, M. Minutillo, S. Di Micco, and E. Jannelli, Design and Costs Analysis of Hydrogen Refuelling Stations Based on Different Hydrogen Sources and Plant Configurations, *Energies* 2022, Vol. 15, No. 2, pp 541, 2022, https://doi.org/10.3390/EN15020541.
6. D. Kondor, Energy storage in hydrogen produced by Plasmalysis (in Hungarian; original title: Energiatárolás plazma-alapú hidrogén előállítással), MSc thesis, Supervisor: A.R. Imre, Budapest University of Technology and Economics, 2023.
7. J. Gianone, Construction of a new geothermal power plant in Hungary in the Southern Great Plain regional (in Hungarian, *Új magyarországi Geotermikus erőmű létesítése a dél-alföldi régióban*), MSc thesis, supervisor: Attila R. Imre, Budapest University of Technology and Economics, 2023.
8. K. Kisari, Economic analysis of the applicability of the Lean model and organizational science aspects in biogas plants (in Hungarian; original title: A Lean-modell alkalmazhatóságának ökonómiai vizsgálata és szervezéstudományi szempontjai biogáz-üzemekben), PhD thesis, Supervisor: I.Takács, Szent István Egyetem, Gödöllő, 2017. https://doi.org/10.14751/SZIE.2017.016.
9. S. Timmerberg, M. Kaltschmitt, and M. Finkbeiner, Hydrogen and hydrogen-derived fuels through methane decomposition of natural gas – GHG emissions and costs, *Energy Conversion and Management: X*, Vol. 7, 2020, https://doi.org/10.1016/j.ecmx.2020.100043.
10. I. Bulfaro, A. Sánchez, G. Benveniste, B. Amante García, and V. J. Ferreira, Environmental, economic, and social impacts of methane cracking for hydrogen production: A comprehensive review, *Int. J. Hydrogen Energy*, Vol. 156, 2025, https://doi.org/10.1016/j.ijhydene.2025.150310.

11. Y. H. Lee et al., Structural transformation of solid carbons produced from the methane pyrolysis process for turquoise hydrogen production, *Int. J. Hydrogen Energy*, Vol. 141, pp 1019–1028, 2025, https://doi.org/10.1016/j.ijhydene.2024.12.377.
12. International Energy Agency, Outlook for Biogas and Biomethane - A global geospatial assessment, 2025, www.iea.org, [Accessed: Aug. 23, 2025].
13. European Parliament and European Council, Regulation on the deployment of alternative fuels infrastructure, and repealing Directive 2014/94/EU - 2023/1804, Sep. 2023, https://eur-lex.europa.eu/legal-content/EN/TXT/?uri=celex%3A32023R1804, [Accessed: Aug. 23, 2025].
14. CEDR Working Group Performance (3.5), Trans-European Road Network, TEN-T (Roads): 2019 Performance Report, Oct. 2020, https://www.cedr.eu/download/Publications/2020/CEDR-Technical-Report-2020-01-TEN-T-2019-Performance-Report.pdf, [Accessed: Aug. 20, 2025].
15. Global Geothermal Power Plant Map | ThinkGeoEnergy - Geothermal News & Insights, https://www.thinkgeoenergy.com/map/, [Accessed: Aug. 20, 2025].
16. M. J. Mayer, B. Biró, B. Szücs, and A. Aszódi, Probabilistic modeling of future electricity systems with high renewable energy penetration using machine learning, *Appl. Energy*, Vol. 336, pp 120801, 2023, https://doi.org/10.1016/j.apenergy.2023.120801.
17. M. Rasool, M. A. Khan, K. Aurangzeb, M. Alhussein, and M. A. Jamal, Comprehensive techno-economic analysis of a standalone renewable energy system for simultaneous electrical load management and hydrogen generation for Fuel Cell Electric Vehicles, *Energy Reports*, Vol. 11, pp 6255–6274, 2024, https://doi.org/10.1016/j.egyr.2024.05.063.
18. National Biomethane-Biogas Green Energy Industry Association, Biogas plants with electricity generation permit, https://biometan-biogaz.hu/biogaz-uzemek/, [Accessed: Aug. 20, 2025].
19. D. I. Permana, D. Rusirawan, and I. Farkas, Waste heat recovery of tura geothermal excess steam using organic rankine cycle, *International Journal of Thermodynamics*, Vol. 24, No. 4, pp 32–40, 2021, https://doi.org/10.5541/ijot.906128.
20. J. Cao et al., Recent progress in organic Rankine cycle targeting utilisation of ultra-low-temperature heat towards carbon neutrality, *Appl. Therm. Eng.*, Vol. 231, 2023, https://doi.org/10.1016/j.applthermaleng.2023.120903.
21. Enogia repurposes idle geothermal wells with compact ORC, ThinkGeoEnergy, https://www.thinkgeoenergy.com/enogia-repurposes-idle-geothermal-wells-with-compact-orc/, [Accessed: Feb. 22, 2026].
22. E. Macchi and M. Astolfi, Organic Rankine Cycle (ORC) Power Systems, Woodhead Publishing, Elsevier, 2017. https://doi.org/10.1016/C2014-0-04239-6.
23. International Renewable Energy Agency, Renewable Power Generation Costs in 2024, Abu Dhabi, 2025, www.irena.org, [Accessed: Aug. 20, 2025].
24. S. R. Patlolla, K. Katsu, A. Sharafian, K. Wei, O. E. Herrera, and W. Mérida, A review of methane pyrolysis technologies for hydrogen production, *Renew. Sustain. Energy Rev.*, Vol. 181, pp 113323, 2023, https://doi.org/10.1016/j.rser.2023.113323.
25. B. J. Leal Pérez, J. A. Medrano Jiménez, R. Bhardwaj, E. Goetheer, M. van Sint Annaland, and F. Gallucci, Methane pyrolysis in a molten gallium bubble column reactor for sustainable hydrogen production: Proof of concept & techno-economic assessment, *Int. J. Hydrogen Energy*, Vol. 46, No. 7, pp 4917–4935, 2021, https://doi.org/10.1016/j.ijhydene.2020.11.079.

26. R. Dagle, V. Dagle, M. Bearden, J. Holladay, T. Krause, and S. Ahmed, An Overview of Natural Gas Conversion Technologies for Co-Production of Hydrogen and Value-Added Solid Carbon Products, U.S. Department of Energy, 2017. https://doi.org/10.2172/1411934.
27. A. Groniewsky, R. Kustán, and A. Imre, Efficiency Increase of Biological Methanation based Power-to-Methane Technology Using Waste Heat Recovery with Organic Rankine Cycle, *Periodica Polytechnica Chemical Engineering*, Vol. 66, No. 4, pp 596–608, 2022, https://doi.org/10.3311/PPCH.20428.
28. A. M. Pantaleo et al., Thermoeconomic optimisation of small-scale organic Rankine cycle systems based on screw vs. piston expander maps in waste heat recovery applications, *Energy Convers Manag.*, Vol. 200, 112053, 2019, https://doi.org/10.1016/j.enconman.2019.112053.
29. Y. Kim and H. Yang, Hydrogen Purity: Influence of Production Methods, Purification Techniques, and Analytical Approaches, *Energies*, Vol. 18, No. 3, 741, 2025, https://doi.org/10.3390/en18030741.
30. A. Król, M. Gajec, J. Holewa-Rataj, E. Kukulska-Zając, and M. Rataj, Hydrogen Purification Technologies in the Context of Its Utilization, *Energies*, Vol. 17, No. 15, 3794, 2024, https://doi.org/10.3390/EN17153794.
31. C. Liu, X. Zhang, J. Zhai, X. Li, X. Guo, and G. He, Research progress and prospects on hydrogen separation membranes, *Clean Energy*, Vol. 7, No. 1, pp 217–241, 2023, https://doi.org/10.1093/CE/ZKAD014.
32. Z. Du et al., A Review of Hydrogen Purification Technologies for Fuel Cell Vehicles, *Catalysts*, Vol. 11, Page 393, Vol. 11, No. 3, pp 393, 2021, https://doi.org/10.3390/CATAL11030393.
33. J. B. S. Hamm, A. Ambrosi, J. G. Griebeler, N. R. Marcilio, I. C. Tessaro, and L. D. Pollo, Recent advances in the development of supported carbon membranes for gas separation, *Int. J. Hydrogen Energy*, Vol. 42, No. 39, pp 24830–24845, Sep. 2017, https://doi.org/10.1016/j.ijhydene.2017.08.071.
34. B. Sasikumar, G. Arthanareeswaran, and A. F. Ismail, Recent progress in ionic liquid membranes for gas separation, *J. Mol. Liq.*, Vol. 266, pp 330–341, 2018, https://doi.org/10.1016/J.MOLLIQ.2018.06.081.
35. G. Bernardo, T. Araújo, T. da Silva Lopes, J. Sousa, and A. Mendes, Recent advances in membrane technologies for hydrogen purification, *Int. J. Hydrogen Energy*, Vol. 45, No. 12, pp 7313–7338, 2020, https://doi.org/10.1016/j.ijhydene.2019.06.162.
36. A. M. Arias, P. L. Mores, N. J. Scenna, J. A. Caballero, S. F. Mussati, and M. C. Mussati, Optimal Design of a Two-Stage Membrane System for Hydrogen Separation in Refining Processes, *Processes*, Vol. 6, Page 208, Vol. 6, No. 11, pp 208, 2018, https://doi.org/10.3390/PR6110208.
37. L. Huang et al., Polymeric membranes and their derivatives for H2/CH4 separation: State of the art, *Sep. Purif. Technol.*, Vol. 297, pp 121504, 2022, https://doi.org/10.1016/J.SEPPUR.2022.121504.
38. European Parliament and European Council, Regulation on the reduction of methane emissions in the energy sector and amending Regulation (EU) 2019/942 - 2024/1787, 2024. https://eur-lex.europa.eu/eli/reg/2024/1787/oj/eng
39. X. He, Techno-economic feasibility analysis on carbon membranes for hydrogen purification, *Sep. Purif. Technol.*, Vol. 186, pp 117–124, 2017, https://doi.org/10.1016/J.SEPPUR.2017.05.034.
40. S. T. B. Lundin, A. Ikeda, and Y. Hasegawa, On the Maximum Obtainable Purity and Resultant Maximum Useful Membrane Selectivity of a Membrane Separator, Membranes (Basel)., Vol. 14, No. 6, pp 143, 2024, https://doi.org/10.3390/membranes14060143.

41. K. Janusz-Szymańska and J. Kotowicz, Energy consumption of the hydrogen separation process from a mixture with natural gas, *Desalination Water Treat.*, Vol. 247, pp 64–71, 2022, https://doi.org/10.5004/DWT.2022.27875.
42. M. Minutillo, A. Perna, and A. Sorce, Combined hydrogen, heat and electricity generation via biogas reforming: Energy and economic assessments, *Int. J. Hydrogen Energy*, Vol. 44, No. 43, pp 23880–23898, 2019, https://doi.org/10.1016/j.ijhydene.2019.07.105.
43. T. Eißler, G. Schumacher, J. Behrens, F. Mendler, and C. Voglstätter, Detailed Cost Analysis of Hydrogen Refueling Costs for Fleets, *Chem. Ing. Tech.*, Vol. 96, No. 1–2, pp 86–99, 2024, https://doi.org/10.1002/cite.202300123.
44. A. Franco and C. Giovannini, Hydrogen Gas Compression for Efficient Storage: Balancing Energy and Increasing Density, Hydrogen, Vol. 5, Pages 293-311, Vol. 5, No. 2, pp 293–311, 2024, https://doi.org/10.3390/hydrogen5020017.
45. SAE International, Fueling Protocol for Gaseous Hydrogen Powered Heavy Duty Vehicles, 2014, SAE International, 400 Commonwealth Drive, Warrendale, PA, United States. https://doi.org/10.4271/J2601/2_201409.
46. K. Reddi, A. Elgowainy, N. Rustagi, and E. Gupta, Impact of hydrogen refueling configurations and market parameters on the refueling cost of hydrogen, *Int. J. Hydrogen Energy*, Vol. 42, No. 34, pp 21855–21865, 2017, https://doi.org/10.1016/j.ijhydene.2017.05.122.
47. R. W. Howarth and M. Z. Jacobson, How green is blue hydrogen?, Energy Sci. Eng., Vol. 9, No. 10, pp 1676–1687, 2021, https://doi.org/10.1002/ese3.956.
48. R. Edwards, J.-F. Larivé, D. Rickeard, and W. Weindorf, Well-to-wheels report version 4.a: JEC well-to-wheels analysis well-to-wheels analysis of future automotive fuels and powertrains in the European context, Luxembourg, Jan. 2014. https://doi.org/10.2790/95629.
49. ENTSOE, ENTSOE Transparency Platform, https://transparency.entsoe.eu/, [Accessed: Aug. 20, 2025].
50. A. Eberle, G. Heath, S. Nicholson, and A. Carpenter, Systematic Review of Life Cycle Greenhouse Gas Emissions from Geothermal Electricity, Denver, Sep 2017, www.nrel.gov/publications, [Accessed: Aug. 20, 2025].
51. European Parliament and European Council, Directive (EU) 2023_2413 of the European Parliament and of the Council, Oct. 2023.
52. B. J. Jesse, G. J. Kramer, V. Koning, S. Vögele, and W. Kuckshinrichs, Stakeholder perspectives on the scale-up of green hydrogen and electrolyzers, *Energy Reports*, Vol. 11, pp 208–217, 2024, https://doi.org/10.1016/j.egyr.2023.11.046.
53. Europe Carbon Black Market - Manufacturers & Companies, https://www.mordorintelligence.com/industry-reports/europe-carbon-black-market, [Accessed: Feb. 22, 2026].
54. H. Legmann, The Bad Blumau geothermal project: a low temperature, sustainable and environmentally benign power plant, *Geothermics*, Vol. 32, No. 4–6, pp 497–503, 2003, https://doi.org/10.1016/S0375-6505(03)00067-1.

Paper submitted: 18.01.2026
Paper revised: 03.03.2026
Paper accepted: 05.03.2026